

NASA Technical Memorandum 84291

AVRADCOM Technical Report 82-A-14

(NASA-TM-84291) HELICOPTER SIMULATION  
VALIDATION USING FLIGHT DATA (NASA) 16 p  
HC A02/MF A01 CSCL 01C

N83-13112

Unclas  
G3/08 02064

---

# Helicopter Simulation Validation Using Flight Data

---

David L. Key, Raymond S. Hanson,  
William B. Cleveland, and William Y. Abbott

---

November 1982



**NASA**  
National Aeronautics and  
Space Administration

United States Army  
Aviation Research  
and Development  
Command



---

# Helicopter Simulation Validation Using Flight Data

---

David L. Key

Raymond S. Hanson, Aeromechanics Laboratory,  
AVRADCOM Research and Technology Laboratories,  
Ames Research Center, Moffett Field, California

William B. Cleveland, Ames Research Center, Moffett Field, California

William Y. Abbott, AVRADCOM Aviation Engineering Flight Activity,  
Edwards Air Force Base, California

**NASA**

National Aeronautics and  
Space Administration

**Ames Research Center**  
Moffett Field, California 94035

United States Army  
Aviation Research and  
Development Command  
St. Louis, Missouri 63166



## HELICOPTER SIMULATION VALIDATION USING FLIGHT DATA

David L. Key  
Chief, Flight Control Division

and

Raymond S. Hansen  
Aerospace Engineer  
Aeromechanics Laboratory  
U.S. Army Research and Technology Laboratories (AVRADCOM)

William B. Cleveland  
Aerospace Engineer  
National Aeronautics and Space Administration  
Ames Research Center  
Moffett Field, California 94035, U.S.A.

William Y. Abbott  
Flight Test Engineer  
U.S. Army Aviation Engineering Flight Activity  
Edwards Air Force Base, California 93523, U.S.A.

### SUMMARY

The paper describes a joint Army/NASA effort to perform a systematic ground-based piloted simulator validation exercise. The subject aircraft is the Army/Sikorsky UH-60A Black Hawk helicopter. The Black Hawk has recently entered service with the U.S. Army, and it is expected that many new roles and missions will evolve that require investigations of flying qualities with simulators. The helicopter has features such as elastomeric main rotor bearings, canted tail rotor, and variable incidence stabilator, all of which provide a challenge in testing, modeling, and verification.

The first step in the procedure was to obtain the best available Black Hawk math model that could be run real-time on the available simulation computer, the CDC 7600. The model is a total force, nonlinear, large angle representation; the rotor description includes rigid blade flapping, lagging, and rotational degrees of freedom. This math model has been programmed for real-time operation and will be checked against the nonreal-time version.

Flight test data were obtained to provide a basis for verifying and improving the math model. Update will be a two-step procedure: first by using engineering judgment based on a knowledge of the model generation assumptions, second by applying state estimation and parameter identification techniques.

The flight tests were performed by the Army Aviation Engineering Flight Activity (AEFA) in response to guidelines from the Aeromechanics Laboratory (AL). Since it is desired to perform analysis with parameter identification techniques, the requirements for instrumentation and calibration were extremely stringent. The tests included extensive trim and static stability points, and special system identification maneuvers as well as steps, doublets, pulses, roll reversals, pull-up and pushovers. Data on pilot performance and control activity were also recorded while performing specially defined mission-type tasks. These will be used in the simulation validation part of the exercise.

Once the math model has been shown to be an accurate representation of the UH-60A, it will be combined with NASA Ames ground-based simulator facilities. The motion base will be the VMS, and the visual system will be a four-window system using computer generated imagery (CGI). Tasks will be "flown" on the ground simulator and pilot subjective data and objective measures will be made to determine and improve the validity of the simulation.

Status of the effort is that the flight tests are complete and the math model has been developed and programmed. Efforts at updating the math model and developing the analytical techniques for assessing the simulator validity/fidelity have been initiated. The simulation portion is scheduled for early 1983.

### 1. INTRODUCTION

A fundamental problem in the use of simulation for aircraft development is that the pilot is required to assess an unknown aircraft. In developing this assessment, he is bound to be influenced by the quality of the simulator itself. Bray (Ref. 1) points out that a sense of realism or subjective fidelity in the simulation flight task is essential and, depending on the research task, some moderate-to-high level of objective or engineering similarity to the flight task is required to obtain this realism. There is no fundamental obstacle to obtaining high objective fidelity in aircraft simulation except in the reproduction of the visual and motion cues. At best, only a small portion of the cues present in an aircraft can be presented, and even this comes at an extremely high cost.

In the application of simulators to pilot training, the large number of facilities involved, and the tendency to maximize the realism of cues available, has led to several studies to determine just how much

# ORIGINAL PAGE IS OF POOR QUALITY

15-2

fidelity is required to train (Refs. 2 and 3). In the use of simulators for handling qualities research, there is a need to understand how the reduced cues influence the research results, or conversely, to define the limitations on use that the limited cues impose for obtaining valid results. The purpose of this paper is to describe a joint Army/NASA program that is making a systematic effort to address this problem.

Rotorcraft pose a particularly difficult problem for simulation technology. The mathematical model required is exceedingly complex so that it takes very large computer capacity to produce real-time solutions for man-in-the-loop simulation. Helicopter mathematical models are also very difficult to verify. The flight characteristics of helicopters tend to have low levels of stability, or be unstable, and there are large interaxis couplings; these are the characteristics which make deprivation in visual and motion cues most critical. Flight phases of particular concern to the Army involve rapid maneuvering flight at very low speed and altitude (Nap-of-the-Earth (NOE) flight). Representing this situation requires wide field-of-view and high detail, which are conflicting requirements that are very difficult to satisfy.

The helicopter chosen as a basis for this research effort is the Sikorsky UH-60A Black Hawk (Fig. 1). This is a modern-technology helicopter that can be expected to be in service with the Army (and probably also the Navy and Air Force) into the next century. It will doubtless have many modifications to satisfy new roles and to incorporate new technology. In addition, the UH-60A Black Hawk is the base helicopter for an Army Research and Development program to demonstrate modern digital flight control technology using fiberoptic components, the Advanced Digital Optical Control System (ADOCS) program. A major part of the ADOCS program involves the development and demonstration of good handling qualities through a range of day and night NOE flight phases, and generation of the appropriate control laws depends to a large extent on adequate simulation of the vehicle. Thus, in addition to the basic techniques and technology that are developed for simulation validation to be applied in general, a validated UH-60A simulation will be a useful end product of this program.

The body of the paper is divided into three main sections. The first discusses in more detail what is meant by the concept of simulator validity and the associated concept of fidelity. The second section describes the process being used to develop and validate the Black Hawk math model, and the final section discusses the approach for assessing the validity of the overall total piloted simulation.

## 2. SIMULATION FIDELITY

Much has been written on the subject of simulator fidelity. Defining the term has been found to be difficult; defining how much fidelity is required for a valid simulation is not currently possible.

An AGARD Working Group, AMP/FMP WG-10, was formed to address the question of how much fidelity is required for pilot training (Ref. 2). The group did not provide an answer to this question but did help clarify the concept and definition of fidelity. In that report, two types of fidelity were defined:

"Objective fidelity (which provides an engineering viewpoint) is the degree to which a simulator would reproduce its real-life in-flight counterpart aircraft, if its form, substance, and behavior were sensed and recorded by an instrumentation system on the simulator.

"Perceptual fidelity (which provides a psychological/physiological viewpoint) is the degree to which the pilot subjectively perceives the simulator to reproduce its real-life counterpart aircraft, in flight, in the operational task situation."

The point is that a distinction is being made between the real cues, which can be measured objectively, and the cues which the pilot subjectively experiences. In selected areas of equipment cues, such as cockpit instrumentation, control panel, and control system operation, the level of objective fidelity can be easily ascertained. In areas of environmental cues, such as visual scenes or motion cueing, extensive data concerning human physiology and cue perception are required. Unfortunately, the knowledge of human physiology is insufficient to determine how much objective fidelity is required to achieve a given level of perceptual fidelity.

Another aspect of fidelity has been hypothesized (Ref. 3). This is to judge the adequacy of perceptual effects by the pilot response behavior (i.e., control strategy and technique) induced by the simulator. The rationale is that if the simulator cannot induce correct technique, then presumably the fidelity is inadequate. With this concept in mind, Ref. 3 defines a concept of fidelity which is:

"The degree to which characteristics of perceivable states induce correct psychomotor and cognitive control strategy for a given task and environment.

"Correct strategy is defined in the task environment; applicable states are chosen on the basis of the specified loop structure essential for performing a task; and characteristics of the states are determined by their role in inducing correct control techniques (i.e., quantification of the loop structure adjustments)."

With this definition, then, a validated simulation could be defined as one in which the characteristics of perceivable states induce correct psychomotor and cognitive control strategy for the given task and environment. It is this concept which is being applied in the current validation effort.

## 3. MATH MODEL VALIDATION

The first step in the overall simulation validation procedure is development of a math model that adequately reproduces the dynamics of the flight vehicle. The approach being taken is to compare flight data with the math model output so that any discrepancies between them can be identified, and then to upgrade the math model. Two basic approaches will be used to update the math model. First, based on engineering insight, and second, by using the parameter identification techniques. This section will outline the form of the math model and the scope and nature of the flight tests, will indicate some of the

correlations obtained, and will discuss the transfer of the model from a nonreal-time to a real-time operating system.

### 3.1 Black Hawk Math Model

The math model to be used as a basis for the real-time simulation was procured from Sikorsky Aircraft. The model is a total system free-flight representation based on the Sikorsky General Helicopter (GENHEL) flight dynamics simulation, and is described in detail in Ref. 4. It is defined at a uniform level of sophistication currently considered appropriate for handling qualities evaluations. The model is also considered to give representative performance trends but does not include the sophisticated aerodynamics necessary to define critical performance characteristics.

The overall structure of the model is presented in Figs. 2 and 3 in functional and block diagram formats, respectively. The basic model is a total force, nonlinear, large-angle representation in six rigid body degrees of freedom. In addition, rotor rigid blade flapping, lagging, and pitch/torsional degrees of freedom are represented. The total rotor forces and moments are developed from a combination of the aerodynamic, mass, and inertia loads acting on each simulated blade. The rotor aerodynamics are developed using a blade element approach where the full range of angle of attack for blade aerodynamics is represented as a function of Mach number. The fuselage is defined by six component aerodynamic characteristics from wind tunnel data which have been extended analytically to large angles. The angle of attack at the fuselage is developed from the free stream plus interference effects from the rotor. These interference effects are based on rotor loading and rotor wake skew angle. The aerodynamics of the empennage are treated separately from the forward airframe to allow good definition of nonlinear tail characteristics. The tail rotor is represented by the linearized closed-form Bailey theory solution.

The Black Hawk flight control system represented in this model covers the primary mechanical and the automatic systems. The latter incorporates the stability augmentation system (SAS), the pitch bias actuator (PBA), the flight path stabilization (FPS) system, and the stabilator mechanization. Figure 4 shows a schematic of the pitch axis. The engine/fuel control model is a linearized representation with coefficients which vary as a function of engine operating condition. The interface between the engine and the rotor module is indicated in the block diagram Fig. 5.

### 3.2 Real-Time Considerations

Rotorcraft math models require certain simplifications and modifications in order to run real-time in a man-in-the-loop simulation (Ref. 5). In nonreal-time the rotor can be represented by the actual number of blades, numerous blade segments, and a small azimuthal advance increment which allows for good definition of blade motion around the azimuth. The computations associated with such a representation cannot be performed real-time even with a very large computer, and an approximation has to be generated with a minimum number of blade segments and the largest rotor azimuth advance increment that will retain satisfactory static and dynamic representation. The form of real-time approximation chosen uses blade segmentation based on equal area annuli to minimize the impact of the approximation. In nonreal-time models, the maximum time step allowable is established based on the computational convergence of rotor flapping which, in turn, depends upon the complexity of blade equations and the rotor rotation rate. A considerable amount of work on the topic of simplifying rotorcraft math models and developing appropriate real-time computation techniques has been performed by McFarland (Ref. 6). These techniques were applied during programming of the Black Hawk model. For this model, a dictating consideration comes from high frequency rotor vibration effects generated by the rotor blade inertial effects in the equations, and the accuracy of the integration of those equations. Using too large a time step will result in an aliasing-like effect whereby higher harmonics of the 4/rev vibration response falls into the low-frequency handling qualities frequency region. An example of this is shown in Fig. 6, taken from some hitherto unpublished work by Mr. R. E. McFarland, NASA Ames. The low-frequency folding effects are clearly seen for  $\Delta t = 0.01$  and  $0.02$  seconds. Such false effects can be eliminated by purging selected inertial terms. An example of the resulting spectrum is also shown in Fig. 6. Tests on the Flight Simulator for Advanced Aircraft (FSAA) show that except at very low frequency, the roll axis motion threshold is greater than the noise level with purged terms. The importance of the very low frequency noise ( $<0.3$  rad/sec) remains to be determined.

### 3.3 Flight Test for Model Validation

The United States Army Aviation Engineering Flight Activity (USAAEFA) at Edwards AFB, California, performed the flight testing in response to requirements laid down by the Army Aeromechanics Laboratory. These requirements included defining the instrumentation and the test matrix required for math model verification and subsequent parameter identification efforts.

#### Instrumentation

Although the helicopter had been instrumented for the Army's airworthiness and flight characteristics testing, the extensive requirements for parameter identification necessitated additional instrumentation and precise calibration. Table 1 lists the instrumentation that was used. Eighty-eight parameters were measured and recorded in a serial PCM stream on magnetic tape with a sample frequency of 100 Hz. Filters of 30 Hz were used on all parameters to insure matching the dynamics and synchronizing the sampling. Some of the more unusual features of the tests are described in the following.

All 3 axes of blade motion (pitch, lead-lag, and flapping) were measured on all 4 rotor blades. Three transducers for each blade were mounted on a special fixture leased from Sikorsky, Fig. 7. Because the transducers were not mounted exactly on the axis of blade motion, a complex transformation was required to resolve the measured angles into true angles.

# ORIGINAL PAGE IS OF POOR QUALITY

15-4

To assist the pilot to perform complex control inputs for the purpose of parameter identification, a real-time visual guide was developed which is similar to that used by the German Aerospace Research and Experimental Establishment, Deutsche Forschungs-und Versuchsanstalt fur Luft-und Raumfahrt (DFVLR). The system consists of an oscilloscope on which the ordinate is scaled in distance of control travel and the abscissa is scaled in time. At the start of a control sequence, a dot showing the current position of the control is superimposed on the input guide and moves right at a rate proportional to time. A trace of actual control input remains superimposed on the input guide at the end of the maneuver so that judgments may be made as to the adequacy of the input. A typical input for parameter identification is a multistep sequence, and an example is shown in Fig. 8. Although the only control inputs requiring the display are for parameter identification, it was found that the display was an excellent quality-control device for all dynamic maneuvers and the static points as well. The display showed inadvertent control movement during trim and indicated the crispness and amplitude of steps, and the timing of pulses.

## Test Matrix and Methodology

Table 2 indicates the scope of the flight tests. These were accomplished in 72 flights with 123 flight hours; approximately half the data were for static points and half were dynamic. All points at a given flight condition were flown at a constant thrust coefficient  $C_T$ , constant  $W/\delta$  and constant  $N/\sqrt{\delta}$  (where  $C_T = T/\rho R^2 (\omega R)^2$ ,  $\delta = \rho/\rho_0$  and  $\theta = T/T_0$ ); this method is described in Ref. 7. Keeping these parameters constant implied that pressure altitude was increased as fuel was burned, and rotor speed was decreased as temperature (speed of sound) was decreased. In some cases, different combinations of  $W/\delta$  and  $N/\sqrt{\delta}$  were used to attain the same value of  $C_T$ , thus attempting to validate the nondimensional concept for this series of tests.

To compensate for center of gravity movement as the fuel was burned, the aircraft was equipped with a movable ballast cart which could travel the length of the aft cabin on a jack screw. The electric motor drive was controlled by the co-pilot according to a predetermined schedule, and its position displayed on the console control panel.

Since the basic unaugmented Black Hawk helicopter is unstable, time histories in response to the various inputs can have very limited duration. Utilizing the SAS would facilitate longer time histories before limits were exceeded, but the SAS characteristics would dominate the response. Since it is the basic helicopter's aerodynamic characteristics that are of interest, the flight tests were flown with the augmentation systems deactivated. In particular, the stabilator was fixed in the nominal position for the test airspeed, the pitch bias actuator was centered and disabled, and the flight path stabilization system was turned off. The SAS was left on for the static points and turned off for the dynamic test points. To minimize time to establish trim, the normal procedure was to have one of the two SAS axes turned on while the pilot established trim and the co-pilot adjusted the test input fixture. As the pilot counted down to the moment of control input, either he or the co-pilot would turn off the remaining SAS axis approximately one second before input. The actual input was made by the co-pilot. Input forms were steps, pulses, doublets, and multistep inputs designed to maximally excite the helicopter without large excursions from trim. Trim was reestablished between inputs and no combined (e.g., pitch and roll) inputs were used.

## 3.4 Correlation with Flight Data

Correlation with two dynamic maneuvers is shown in Figs. 9 and 10. The math model response was computed using the actual flight measured control positions. In order to account for the differences in the flight measured and model predicted control positions in trim, only the deviation from trim is introduced as the forcing input. Both the flight data and the simulation data were filtered using identical zero phase shift filters in order to suppress the high frequency vibration characteristics. This enables an easier comparison of the frequencies of interest to the flight dynamicist.

In Fig. 9, the pilot's collective stick input was used to drive the math model. The first plot demonstrates a comparison of the measured collective pitch of the main rotor, and the output of the simulation, indicating some differences in the control system rigging. A comparison of the measured rotor response (coning) shows good agreement initially, but tends to diverge in the long term, indicating that the model is more unstable than the flight vehicle. The coning response can be seen to be a major contributor to the normal acceleration of the aircraft. The vertical velocity shows considerable discrepancies which are directly attributable to the errors in the predicted normal acceleration. Figure 9 illustrates a need for a systematic approach to upgrading the model, working from the input to the highest level of integration down to the lowest order state.

Figure 10 shows the response to a lateral stick input. There exists reasonably good correlation with the rotor response (lateral flapping); however, some discrepancies are evident in the roll rate which strongly affect the predicted roll attitude. It may also be noted that the trim longitudinal stick position predicted by the model does not agree with the flight value. A comparison of the responses in the off-axes (pitch and yaw) is also provided.

## 3.5 Parameter Identification

The motivation for the parameter identification effort is to develop a systematic and semi-automated procedure for upgrading the math model, and eliminating discrepancies such as those shown in Figs. 9 and 10. The approach being taken is somewhat different from normal because the model used for the identification is a nonlinear blade element model, and the parameters being identified are the actual physical parameters (i.e., lift curve slope, interference factors, etc.) that are present in the nonlinear equations of motion. The approach normally taken by helicopter analysts is to identify the coefficients in a model linearized about a given operating point (i.e., stability derivative extraction). The approach being taken in this project is thought to have several advantages, the most important of which is that the model is being validated over a large portion of the flight envelope rather than at one isolated operating or trim condition. This approach allows for the processing of trim and static stability data in the identification process, as well as large disturbance transient maneuvers. The approach also provides for direct

correlation and improvement of an operational simulation model without the intermediate steps that would be necessary if stability derivatives were used as the basis of comparison. On the other hand, several disadvantages must be considered. The problem is a computationally complex and highly nonlinear optimization problem and, as such, requires a reasonably accurate *a priori* model to allow correct convergence. Further, use of an output error algorithm is mandatory due to the difficulties in developing an extended Kalman filter algorithm for use with a blade element type model. Use of an output error algorithm does not allow for process noise effects which implies knowledge of a perfect model structure, and does not allow for unknown external disturbances.

The number of parameters in the nonlinear parameter identification is not appreciably more than that encountered in a fully coupled rotor and body linear problem. However, the table look-up data must be parameterized in such a way as to allow for identification of errors within the tables. Further, the actual parameters identified in a given identification run must be reduced to a manageable subset that is consistent with the maneuvers and/or static data being processed.

Development of the software to perform this automated model upgrade is currently under way. The basic concept behind this computer program is shown in Fig. 11.

#### 4. SIMULATOR VALIDATION

As defined in Section 2, the basis of assessing simulator validity will be to assess the extent to which the characteristics of the perceived states induce correct psychomotor and cognitive control strategy for the given task and environment.

The correct psychomotor and cognitive control strategies are those achieved in flight in the actual helicopter. To determine these strategies, special-mission type flight testing was performed concurrently with the parameter identification tests described in the previous section. A series of mission flight phases (Table 3) were performed. These consisted of a series of flight task segments which included basic manual regulation of flight condition (hover, cruise, descent, etc.) as well as various discrete maneuvers (takeoff, acceleration, deceleration, quick-stop, etc.). In each case the pilot was instructed to demonstrate a good representative example of the flight task execution. Generally, this was based on the existing task descriptions and performance standards given in the utility helicopter aircrew training manual.

The recording system used for the parameter identification work was also used in the mission flight tests. No additional data, such as video recording of pilots' activity or eye point of regard, was available for these tests. To provide sufficient data base with which to generalize, it was important to have maneuvers repeated both by the same pilot and by different pilots. Primary emphasis was placed on NOE point-to-point, dash-quick-stop, bob-up, sideways mask, dolphin, and slalom. All of these tasks were flown at least twice by two pilots.

##### 4.1 Mission Flight Test Data Analysis

The basis for data analysis is that the control strategy from the simulator should match that from flight test. A pilot strategy for controlling the task is hypothesized, and the flight data used to determine the parameters by a least squares regression fit. A closed-loop pilot aircraft model is hypothesized for each task, certain parameters in the pilot model can be assumed based on past experimental analysis, and the flight data are then used to determine the unknown parameters. This effort is being performed under contract by Systems Technology, Inc., and the approach is described in Ref. 3. Each flight task maneuver has to be modeled at its most elemental level. Thus, if the task is longitudinal in nature, the lateral portion is deleted. The model represents the pilot's control, his perception, and the helicopter plant dynamics. Figure 12 shows a block diagram comparing the situation in the simulator with that for the real aircraft. In practice, considerable skill is required to get an adequate model of these control loops. The aircraft model is obtained first by using the appropriate transfer function of aircraft response to input. Inner or high frequency loops, such as attitude control, and outer loops, such as speed and altitude control, and the appropriate cue information being used by the pilot have to be hypothesized. The parameters in these various loop closures are determined by performing linear regression fits on the actual flight time histories. By using several pilots and repeated aircraft or simulator flights, it is hoped to develop confidence in the resulting closed-loop models.

Flight test data to perform this phase of the analysis have only recently become available and so the task of generating the appropriate loop closures has only just begun; however, a preliminary analysis of a hovering turn will be described to illustrate the methodology.

##### 4.1.1 Pilot Strategy Evaluation for Hovering Turns

Two hovering turns, one to the left and one to the right, have been analyzed to develop the pilot strategy. Time histories for the turns are shown in Fig. 13.

The pilot strategy for the hovering turns can be broken down into two segments. The first segment involves starting and maintaining the turn; the second segment involves stopping the turn, and regulating yaw rate and heading error to obtain the desired heading. In initiating the hover turn, the pilot's heading error is large (for these cases, approximately 90°), and, therefore, the feedback of this parameter is not of primary importance. Instead, the pilot puts a high priority on increasing, and subsequently maintaining, an acceptable yaw rate. As long as the heading error is greater than 10° to 15°, the pilot will try to maintain some limit yaw rate depending on the aggressiveness of the turn. As heading error is reduced to the 10° to 15° range, the pilot will shift his primary feedback emphasis back to heading error, and yaw rate will be adjusted as required to line up the nose of the helicopter with the desired heading. The control law that provided the best representation of these maneuvers is represented in Fig. 14 and has the difference equation form:

$$\delta p = K_p \delta p Z^{-2} + K_v \psi_a Z^{-1} + K_{\psi_a} \psi_a Z^{-1} + \text{BIAS}$$

In the first segment of the turns the heading feedback was limited to an effective constant yaw rate command, and  $1p_{\psi}$  was determined to be as indicated in Fig. 14. Frequency responses for this transfer function are shown in Fig. 15. Overall, the pilot model suggests a bandwidth requirement of approximately 0.1 rad/sec for initiation of the turn maneuver. Using these solutions for  $Y_{p_{\psi}}$  and the flight values of  $\psi$ , the  $\delta p$  was computed and compared with the flight value (Fig. 16).

The pilot controller elements for the second segment of the maneuver involves closing the outer loop of heading angle as well as the use of yaw rate in the inner loop. The values obtained for the coefficients for the second segment of both turns are shown in Fig. 14. Inspection of the maneuver time histories (Fig. 13) indicates that the gain and bandwidth of the  $Y_{p_{\psi}}$  controller should be significantly greater than that required for initiation of the turn. This is further reinforced by the logical conclusion that it should be a more difficult task for a pilot to trim out on a new heading angle than for the pilot to initiate a simple heading change. Figure 17 presents a summary of the frequency response gain and phase results for the second segment of both turns. For the nose left turn, the break frequency occurs at approximately 1.1 rad/sec; the right turn break frequency is approximately 0.55 rad/sec. The difference between the two values could be partially explained by the significantly greater magnitude of control activity required by the pilot to close on the desired left turn heading when compared with the right turn. In making a left turn, the pilot must overcome the main rotor torque by increasing tail rotor thrust, whereas a right turn is produced by reducing tail rotor thrust. This puts the tail rotor into a different operating condition and may cause differences in the pilot control. Overall, the pilot model suggests an approximate bandwidth of 1.0 rad/sec for the tracking task of concluding the turn at a specified new heading. Control activity for both of these maneuvers was reconstructed using the pilot model, and the results are compared with flight in Fig. 18. As for the initiation of the turn, the results indicate that the pilot model is a realistic representation.

#### 4.2 Simulation Evaluation

In the simulator testing, the closed-loop pilot models obtained from analysis of the flight test data will be combined with a model of the simulator that represents the perceived and used visual and motion cues (Fig. 12). It is hypothesized that differences in control strategy between the simulator and flight are due to the simulator components themselves, and the analytical approach will be to attempt to account for these differences by appropriate modeling of the visual and motion cues. The simulator testing will, therefore, consist of repeating the mission flight phases performed in flight with the simulator in its basic configuration, and also with reduced visual and motion cues.

The simulator facility to be used will consist of a helicopter cockpit having a wide field-of-view visual display with a computer generated imagery (CGI) visual scene, mounted on the NASA Ames vertical motion simulator (VMS), a large amplitude motion generator. The VMS is shown in Fig. 19, and a typical CGI scene is shown in Fig. 20 superimposed over the actual field-of-view of the Black Hawk. Table 4 shows the most pertinent performance specifications of the VMS and also lists some performance requirements (Ref. 8). The VMS capabilities are considered to be excellent for NOE flight, especially in the rotational and vertical axes, and most of the requirements of Ref. 8 have been met. Important parameters in the visual display are the field-of-view, the resolution, the level of detail, and the overall dynamics. As can be seen from Fig. 20 the four-window CGI does provide a significant field-of-view relative to the Black Hawk, and the CGI data base shown has subjectively good detail. The resolution is 6.0 arc minutes per line pair. Dynamics of the CGI system are 30 per second update rate, the picture refresh rate is 60 per second, and total delay for a scene computation change is 100 milliseconds.

The sensitivity testing portion of the simulator validation exercise will involve repeating the flight tasks with various degraded combinations of the simulator equipment. Variations in motion will be from full to 50% travel, and will also use the hexapod portion only. Use of the hexapod only is included to allow some comparison with most civil and military flight trainers which use such devices. The visual simulation parameters to be changed are field-of-view, which will be reduced from four to three to two and one windows, and display dynamics, which will be evaluated by the use of time delay compensation techniques. The technique to be used is described by Crane in Refs. 9 and 10.

It is expected that the simulator testing will be performed during the spring of 1983.

#### 5. CONCLUSIONS

The paper describes a systematic effort to generate techniques for simulator validation. This is a complex task and involves considerable effort and the skills of several organizations.

Efforts so far have resulted in procuring and programming a basic math model, and performing flight tests to obtain the data on which to base an update. In addition, some of the parameter identification tools required to handle the data have been developed. To overcome the difficulty of quantifying perceptual fidelity, the validation effort will be based on the concept that pilot control strategy in the simulator should match the control strategy used in flight. Flight data have been obtained to use as a basis for developing models of control strategy during mission-related tasks.

Currently, work is proceeding on the model update; a contract has been issued to Sikorsky to use the flight data to identify deficiencies and make improvements in their basic math model. In-house efforts are continuing to develop and apply state and parameter identification techniques to improve the structure of the model and refine the parameters. Systems Technology, Inc. is working under contract to use the flight data to develop analytical models for control strategy and accommodate the effects of the simulator components.



The future plans are to incorporate the updated model into a NASA real-time simulator facility during 1983. At that time, data will be obtained to perform the final step in the validation assessment analysis.

6. REFERENCES

1. Bray, Richard S., "Helicopter Simulation Technology: An Ames Research Center Perspective." p. 199, NASA CP 2219, Helicopter Handling Qualities, April 1982.
2. Key, David L. (Ed.), "Fidelity of Simulation for Pilot Training." AGARD Advisory Report No. 159, October 1980.
3. Heffley, Robert K. et al., "Determination of Motion and Visual System Requirements for Flight Training Simulators." System Technology, Inc., TR 1162-1, August 1981.
4. Howlett, J. J., "UH-60A Black Hawk Engineering Simulation Program Mathematical Model." NASA CR 166309, December 1981.
5. Cooper, D. E., and Howlett, J. J., "Ground Based Helicopter Simulation." Paper presented at AHS Symposium on Status of Testing and Model Techniques for V/STOL Aircraft, October 1972.
6. McFarland, R. E., "Establishment of a Rotor Model Basis." NASA TP-2026, AVRADCOM TR-81-A-14, June 1982.
7. Boirun, B. H., "Generalizing Helicopter Flight Test Performance Data." AHS Annual National Forum, May 1978.
8. Sinacori, John B., "The Determination of Some Requirements for a Helicopter Flight Research Simulation Facility." Systems Technology, Inc., TR 1097-1, September 1977.
9. Crane, D. F., "Time Delays in Flight Simulator Visual Displays." Proceedings of the 1980 Summer Computer Simulation Conference, Seattle, Washington.
10. Crane, D. F., "Flight Simulator Visual Display Compensation." Proceedings of the 1981 Winter Simulation Conference, Atlanta, Georgia, December 1981.

TABLE 1. FLIGHT TEST INSTRUMENTATION

<u>Inertial/ground reference</u>	<u>Control system</u>	<u>Main rotor</u>
C.g. accelerometers (3 axes)	Pilot control positions	Blade flapping (4 blades)
Nose accelerometers (3 axes)	Swashplate position	Blade lead-lag (4 blades)
Angular rate gyros (3 axes)	Tail rotor pitch	Blade pitch (4 blades)
Vertical gyro	Stabilator position	Rotor rpm
Direction gyro	SAS servo outputs	Rotor azimuth
Angular accelerometers (3 axes)	Mixer inputs	Main rotor shaft bending
Radar altimeter	Pitch bias actuator position	Main rotor torque
Magnetic heading	Primary servos position	
<u>Engines (both)</u>	<u>Air data</u>	
Power turbine speed	Angle of attack	
Gas generator speed	Angle of sideslip	
Fuel flow rate	Airspeed	
Engine torque	Barometric altitude	
	Total air temperature	
	Low airspeed system	

TABLE 2. SCOPE OF TEST MANEUVERS

Static	Dynamic
<u>Level flight</u> - 5 longitudinal CGs, 3 lateral CGs, 4 Cys using 6 combinations of W/s and N/v/s, stabilator sweeps, and rotor speed sweeps, all at a minimum of 4 airspeeds, including hover.	<u>Step inputs</u> - All axes (longitudinal, lateral, pedal, and collective), both directions, 2 CGs, 4 airspeeds including hover, varying magnitude.
<u>Low speed</u> - Forward, rearward, and lateral at 2 CGs and 2 Cys to 40 knots.	<u>Pulse inputs</u> - All axes, both directions, 4 airspeeds including hover.
<u>Climbs and descents</u> - 2 CGs, 2 Cys with variations, 3 airspeeds, 2 rates of climb, and 2 rates of descent each.	<u>Doublets</u> - All axes, both directions, 2 CGs, 2 Cys with variation, 2 airspeeds including hover, varying magnitude.
<u>Level turns</u> - 3 airspeeds, 2 CGs, 2 angles of bank in both directions.	<u>System identification inputs</u> - All axes, both directions, 2 CGs, 3 airspeeds, varying magnitude.
<u>Wind-up turns</u> - 2 airspeeds, 2 g levels in both directions.	<u>Roll reversals</u> - Both directions, 2 airspeeds.
<u>Hover</u> - 5 IGE hover heights.	<u>Sideslip reversals</u> - One airspeed, both directions.
<u>Static longitudinal stability</u> - 2 CGs, 3 Cys with variations, 2 rotor speeds, climbs and descents, at 3 airspeeds each.	<u>Long term response</u> - 3 airspeeds, both directions.
<u>Lateral-directional stability</u> - Same as longitudinal stability.	<u>Pushovers and pullups</u> - 2 airspeeds, both directions, varying magnitude.

TABLE 3. MISSION FLIGHT TASKS

Takeoff/landing tasks in an airport environment

1. Takeoff to hover
2. Hover
3. Hover turns
4. Taxiway flight
5. Right sideward acceleration/deceleration
6. Left sideward acceleration/deceleration
7. Rearward acceleration/deceleration
8. Normal takeoff
9. Maximum performance takeoff
10. Traffic pattern flight
11. Approach to hover
12. Landing from hover

Level/climb/descent flight tasks

1. Straight and level flight
2. Climb at specified airspeed and rate of climb
3. Level flight turns
4. Descents at specified airspeed and rate of climb
5. Single engine approach and roll on landings
6. Autorotations to the runway followed by power recovery

NOE/contour/low level flight tasks

1. NOE terrain flight takeoff
2. Low-level flight
3. Contour flight
4. NOE flight
5. NOE pop-up
6. NOE bob-up (mask/unmask at hover)
7. NOE side unmask
8. NOE dash followed by quickstop along a straight line and with a turn
9. NOE hard break sideward
10. NOE hard turn
11. NOE slalom maneuver
12. NOE dolphin maneuver
13. Confined area approach and landing

TABLE 4. COMPARISON OF NOE SIMULATOR MOTION REQUIREMENTS AND VMS PERFORMANCE

Axis	Position rad,m		Velocity rad/sec, m/sec		Acceleration rad/sec <sup>2</sup> , m/sec <sup>2</sup>		Frequency response, bandwidth, rad/sec	
	Required	VMS	Required	VMS	Required	VMS	Required	VMS
Roll ( $\phi$ )	$\pm 0.3$	$\pm 0.38$	$\pm 0.5$	$\pm 0.26$	$\pm 1$	$\pm 0.87$	20	0.4-20
Pitch ( $\theta$ )	$\pm 0.3$	$\pm 0.45$	$\pm 0.5$	$\pm 0.26$	$\pm 1$	$\pm 0.87$	20	0.4-20
Yaw ( $\psi$ )	$\pm 0.4$	$\pm 0.51$	$\pm 0.6$	$\pm 0.26$	$\pm 1$	$\pm 0.87$	20	0.4-20
Longitudinal (X)	$\pm 1.3$	$\pm 0.8$	$\pm 1.3$	$\pm 0.6$	$\pm 3$	$\pm 4.9$	20	0-0.2
Lateral (Y)	$\pm 3$	$\pm 6$	$\pm 2.6$	$\pm 3$	$\pm 3$	$\pm 7.3$	20	0-20
Vertical (Z)	+7, -14	$\pm 9$	+8, -11	$\pm 6$	+14, -12	$\pm 9.8$	20	0.2-12



Figure 1. UH-60A Black Hawk.

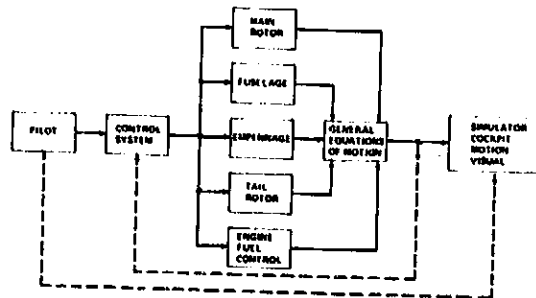


Figure 3. Math model simplified block diagram.

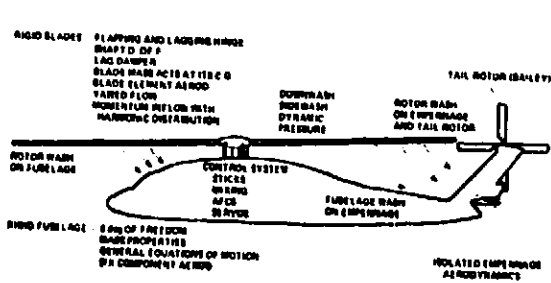


Figure 2. Math model features.

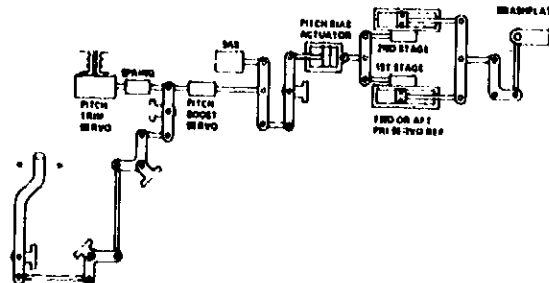


Figure 4. Pitch flight controls schematic.

15-10

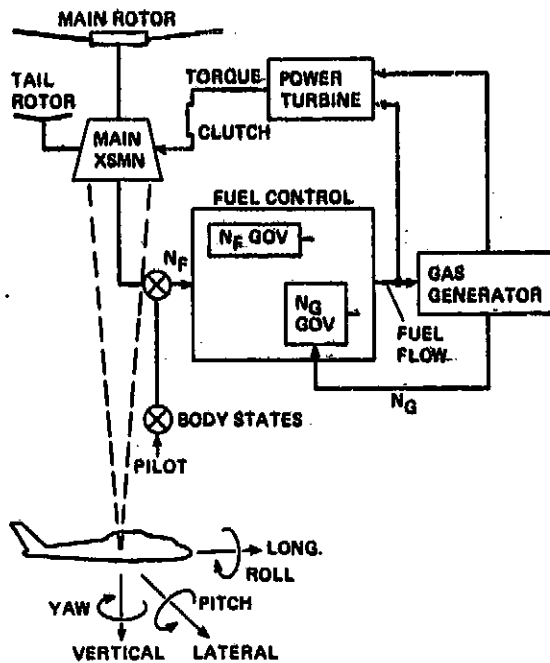


Figure 5. Engine integration into math model.

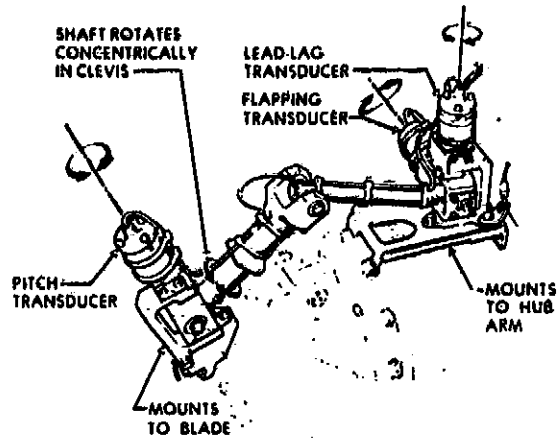


Figure 7. Blade angle measurement fixture.

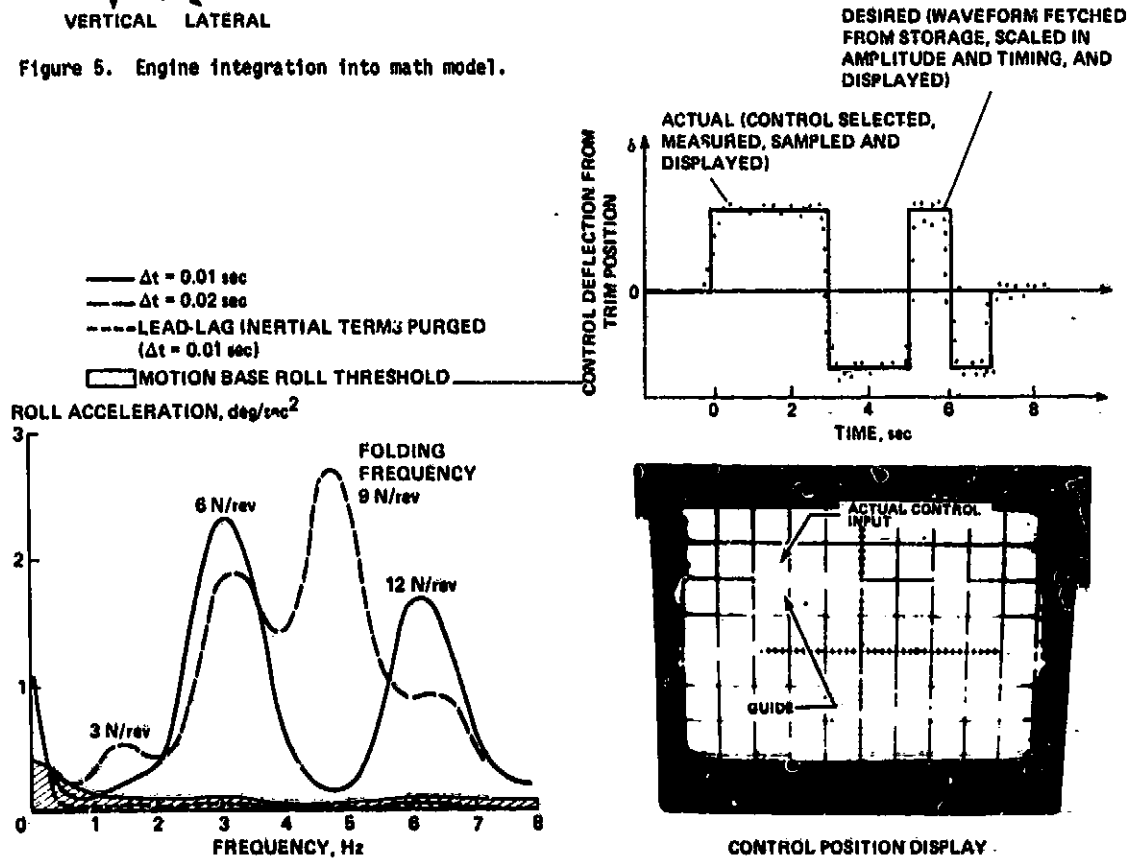


Figure 6. Power spectrum of rolling moments at 100 knots, trim.

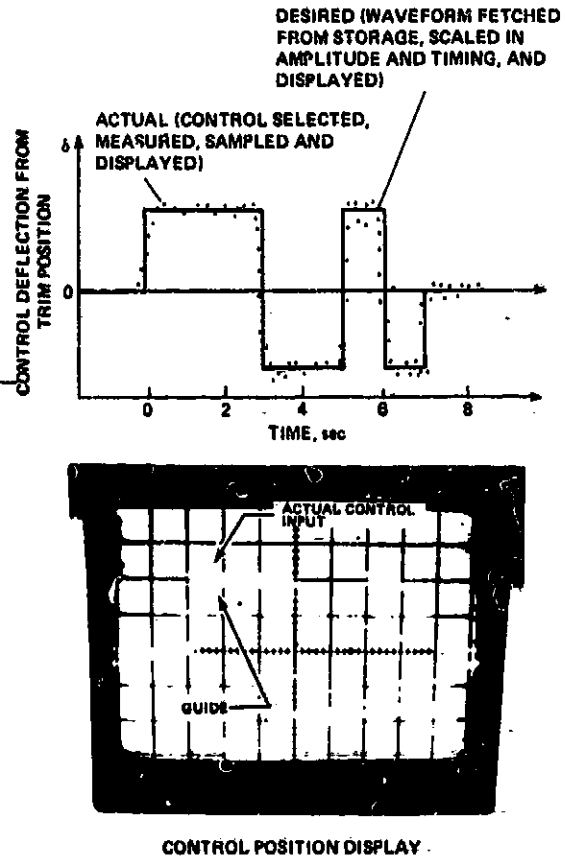


Figure 8. Input form and pilot's display.

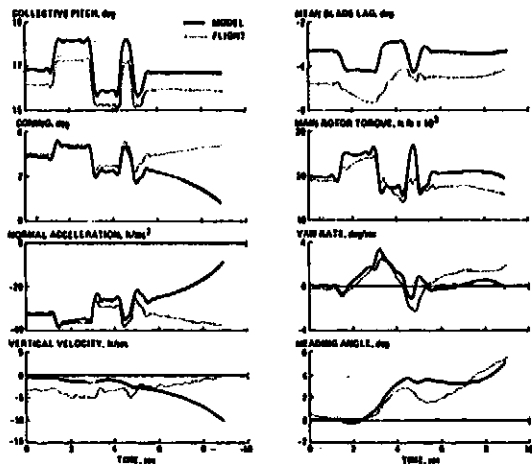


Figure 9. Collective stick input, 60 knots.

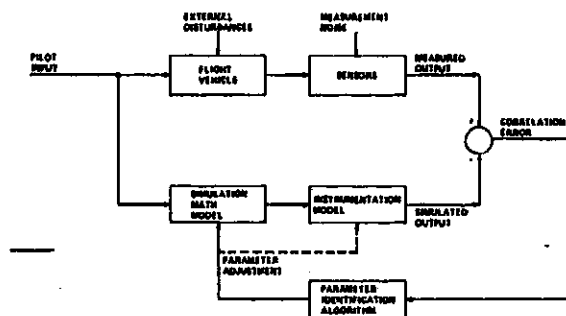


Figure 11. Parameter identification concept.

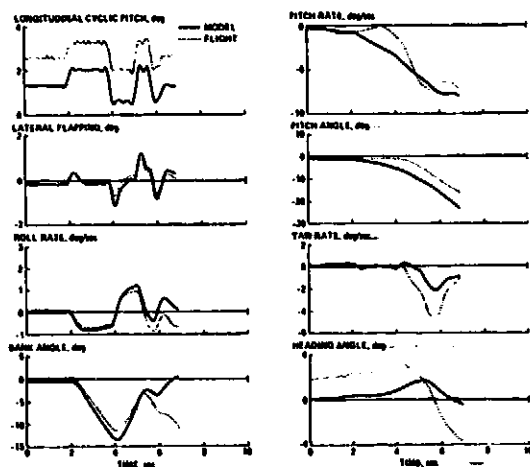


Figure 10. Lateral stick input, 60 knots.

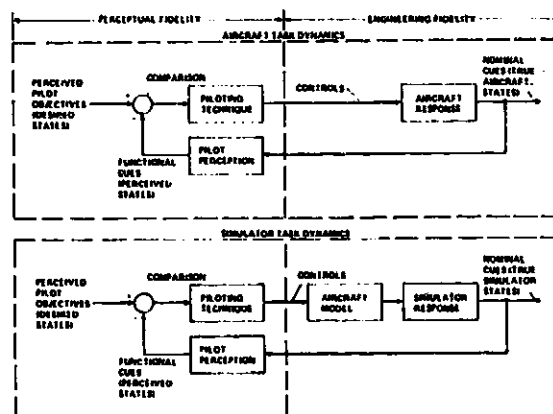


Figure 12. Flight task components in helicopter and simulator.

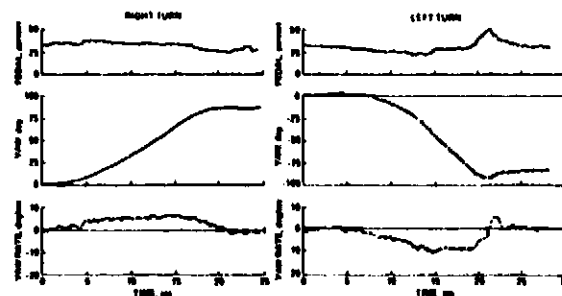
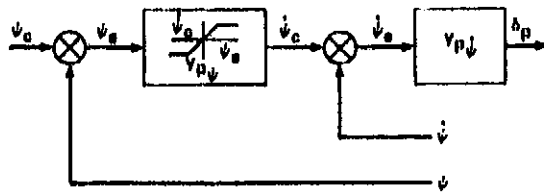


Figure 13. Time history for hovering turns.

ORIGINAL PAGE #1  
OF POOR QUALITY

15-12



	LEFT TURN	RIGHT TURN
FIRST SEGMENT		
$K_{\delta_p}$	0.98	0.93
$K_{\dot{\psi}_e}$ (percent-sec/deg)	0.086	0.075
SECOND SEGMENT		
$K_{\delta_p}$	0.78	0.89
$K_{\psi_e}$ (percent/deg)	0.56	0.12
$K_{\dot{\psi}_e}$ (percent-sec/deg)	0.32	0.25

$$Y_{p\dot{\psi}} = \frac{K_{\dot{\psi}_e}}{-K_{\dot{\psi}}}$$

$$Y_{p\dot{\psi}} = \frac{-K_{\dot{\psi}}}{1 - K_{\delta_p} s^{-2}}$$

Figure 14. Pilot control strategy in hovering turn.

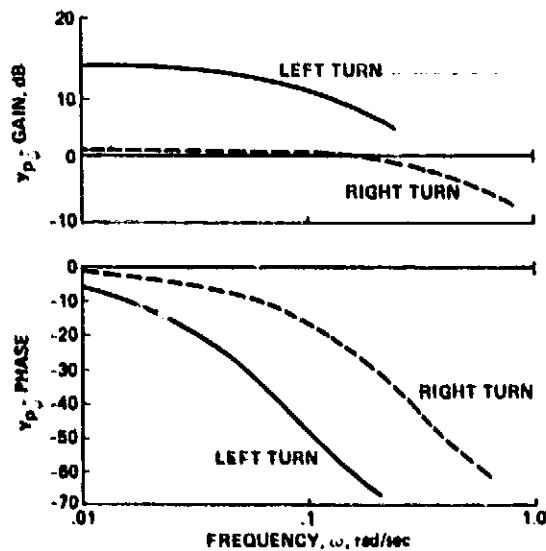


Figure 15. Frequency response for  $Y_{p\dot{\psi}}$  (initial part of turn).

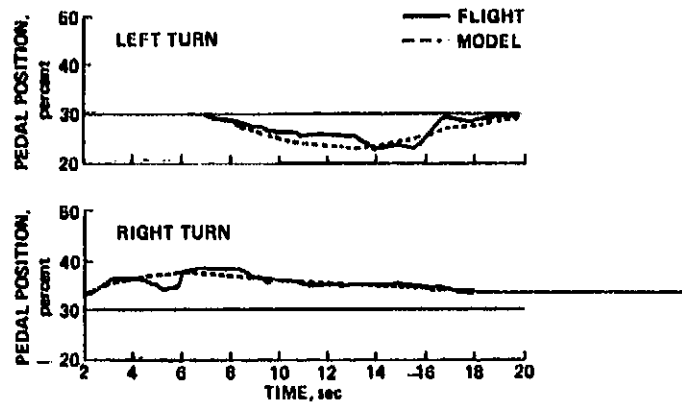


Figure 16. Control usage for initial part of the hovering turn.

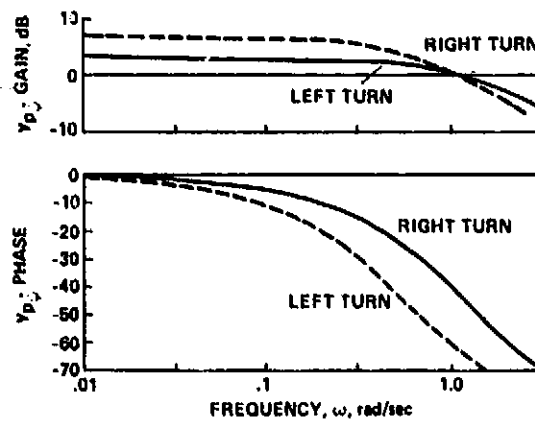


Figure 17. Frequency response for  $Y_{p\dot{\psi}}$  (second part of turn).

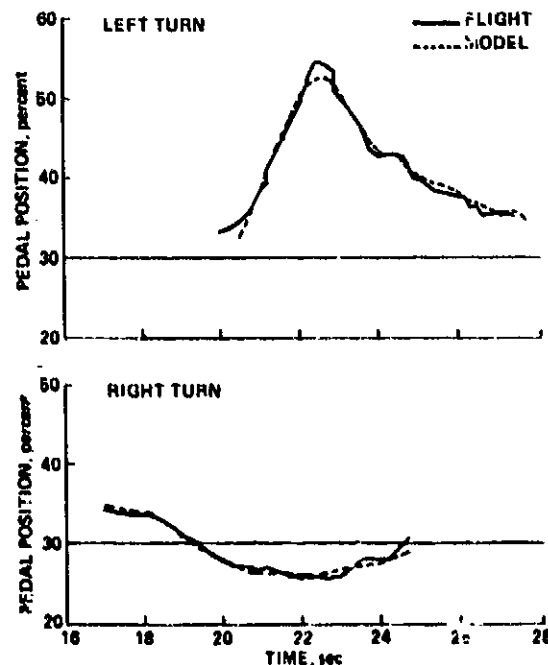


Figure 18. Control usage for second part of hovering turn.

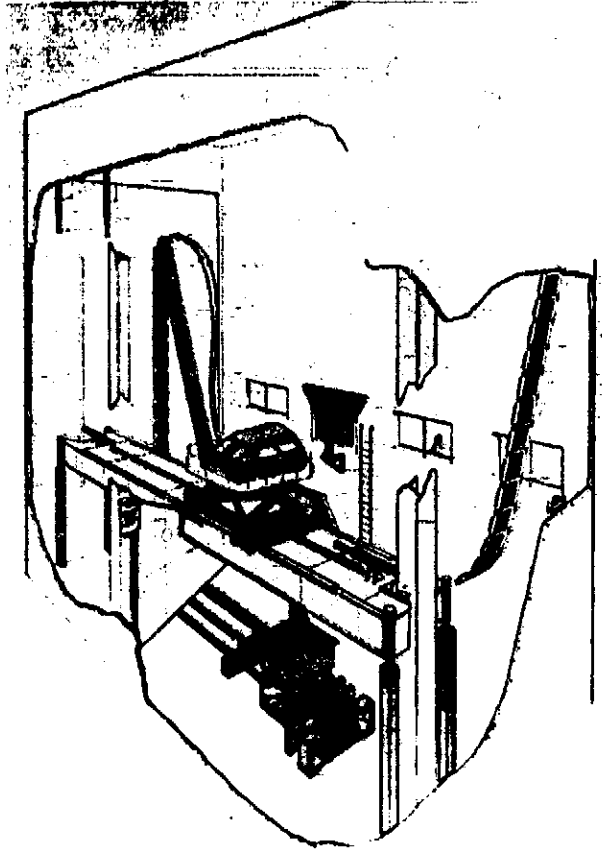


Figure 19. Vertical motion simulator (VMS).

I-CAB CRT LOCATIONS ON UH-60 FOV

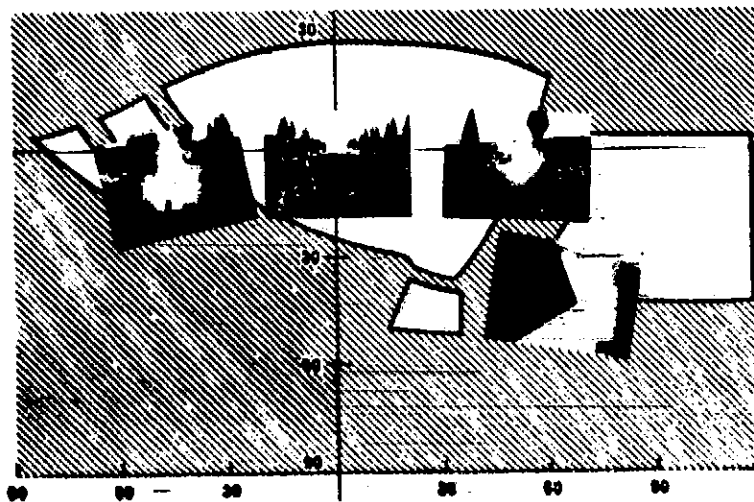


Figure 20. CGI four-window display.